The EMBO Journal vol.15 no.2 pp.226–235, 1996

The ATP binding cassette transporter ABC1, is required for the engulfment of corpses generated by apoptotic cell death

Marie-Françoise Luciani and Giovanna Chimini[1]

Centre d'Immunologie INSERM CNRS de Marseille-Luminy, Parc Scientifique de Luminy, Case 906, 13288 Marseille Cedex 9, France

[1]Corresponding author

ATP binding cassette (ABC) transporters define a family of proteins with strong structural similarities conserved across evolution and devoted to the translocation of a variety of substrates across cell membranes. A few members of the family are known in mammals, but although all of them are medically relevant proteins, knowledge of their molecular function remains scanty. We report here a morphological and functional study of the recently identified mammalian ABC transporter, ABC1. Its expression during embryonic development correlates spatially and temporally with the areas of programmed cell death. More specifically, ABC1 is expressed in macrophages engaged in the engulfment and clearance of dead cells. Moreover, ABC1 transporter is required for engulfment since the ability of macrophages to ingest apoptotic bodies is severely impaired after antibody-mediated steric blockade of ABC1. A structural homologue of ABC1 has been identified in the *Caenorhabditis elegans* genome and maps close to the *ced-7* locus. Since *ced-7* phenotype is precisely defined by an impaired engulfment of cell corpses, it is tempting to surmise that ABC1 might be a mammalian homologue of *ced-7*.

Keywords: ABC transporters/apoptosis/engulfment

Introduction

ATP binding cassette (ABC) transporters constitute a large family of evolutionary conserved transmembrane proteins involved in the transport of a wide variety of substrates across cell membranes (for review see Higgins, 1992; Doige and Ames, 1993). Although a large number of transporter/substrate pairs have been identified in bacteria, in eukaryotes only a few members of the family are known and scant information is available about their physiological function or their physiological substrates. The only exception is the yeast STE6 transporter whose function as catalyst of the unconventional secretion of *a* factor has been established unambiguously (McGrath and Varshavsky, 1989).

However, most of the mammalian ABC transporters have been associated with clinically relevant phenotypes. The P-glycoproteins are responsible for the multi-drug resistance developed by tumours during therapy both *in vivo* and *in vitro* (Gottesman and Pastan, 1992) and the physiological function of one of the isoforms has recently been related to transmembrane translocation of phosphatidylcholine (Smit *et al.*, 1993; Ruetz and Gros, 1994). CFTR dysfunction is the basis of cystic fibrosis (Riordan *et al.*, 1989) and the two peroxisomal ABC transporters are involved in the pathogenesis of two major genetic disorders, the Zellweger syndrome and adrenoleukodystrophy (Gartner *et al.*, 1992; Mosser *et al.*, 1993; Valle and Gartner, 1993). Finally, genetic defects in the TAP transporters which are required for the presentation of endogenous antigens by HLA class I molecules has been recently reported as the molecular basis of a bare lymphocyte syndrome type I phenotype (De la Salle *et al.*, 1994).

We have recently described the characterization of two novel mammalian members of the family of ABC transporters, ABC1 and ABC2 (Luciani *et al.*, 1994), for which no physiological function is known so far.

In this paper we analyse the developmental expression pattern of the ABC1 transporter, by *in situ* hybridization and immunohistochemistry on mouse embryo sections. ABC1 shows discrete localization in areas of developmental cell death, in particular the interdigital zone in the developing limb. In the interdigital webs ABC1 appears to be expressed in the macrophages involved in the engulfment of apoptotic cells. Engulfment of cells undergoing cell death requires a functional ABC1 transporter since antibody-mediated blockade severely impairs the phagocytic ability of *ex vivo* macrophages. Finally, an ABC1 structural homologue has been identified in the *Caenorhabditis elegans* genomic region spanning the *ced-7* locus (Wilson *et al.*, 1994; A.Coulson, personal communication). *Ced-7* loss of function phenotype results in impaired engulfment of cells undergoing developmental cell death (Ellis *et al.*, 1991a,b). Co-localization and the similarity of function suggest that ABC1 and *ced-7* might be a pair of homologous genes. They could then provide an additional example at the engulfment stage of the striking conservation across evolutionary distant species of the genes controlling multiple aspects of the death programme.

Results

The developmental expression pattern of ABC1 transporter correlates with the occurrence of programmed cell death

To gain insight into the function of ABC1, we started an analysis of its expression during embryonic development in mouse. A preliminary Northern blot analysis on RNA extracted from whole mouse embryos aged from day 7.5 to 17.5 (E7.5 to E17.5), allowed us to establish that ABC1 expression is detectable throughout the examined time period (Figure 1A).

A more detailed investigation was then carried out by

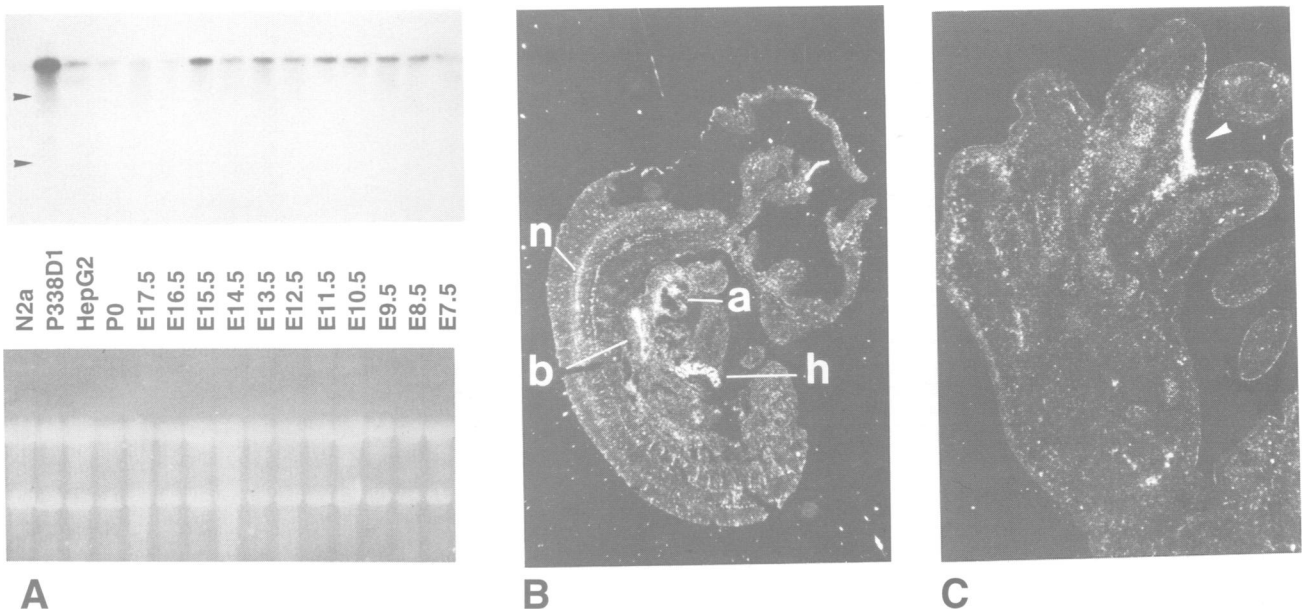

Fig. 1. *ABC1* is expressed during embryonic development. (**A**) Northern blot analysis on total RNA from whole embryos (E 7.5–E17.5) at birth (P0) and a few reference cell lines: P388D1, murine monocyte macrophage; N2a, murine neuroblastoma; HepG2, human hepatoma. Top panel: hybridization with ABC1-specific probe; arrowheads mark 28S and 18S. Bottom panel: ethidium bromide staining of the gel before transfer. (**B**) ABC1 *in situ* hybridization on sagittal cryosections from E11.5 embryos. The liver anlage (h) is visible. b, mesenchyma surrounding the bronchi; a, region of the aortic arches; n, neural tube. a discrete positivity is seen in the ventral region, which extends longitudinally. (**C**) ABC1 transcript is expressed in the interdigital zone of the limb bud. Parasagittal cryosections of E13.5 mouse embryos were hybridized with the complementary ABC1 cRNA probe. The signal is highlighted by an arrowhead.

in situ RNA hybridization on cryosections obtained from E10.5 to E15.5 mouse embryos. The cRNA probe was transcribed from the same template used for Northern hybridization, corresponding to the central region of the full-length cDNA and specifically detecting ABC1 transcript. Serial sections were hybridized with the complementary antisense probe and the homologous sense probe in order to ascertain the specificity of the detected signal.

Two classes of signals could be distinguished on the basis of their temporal profile. The first group corresponds to embryonic areas which express the ABC1 transcript from the onset of their morphological differentiation and throughout the examined time period (Kaufman, 1992). The liver anlage at the septum transversum is ABC1-positive as soon as E10; this hepatic expression increases further by E11.5 (Figure 1B) and remains constant between E13.5 and 15.5. By E11.5 the mesenchymal tissue surrounding the neural tube, where differentiation of the enveloping membranes is taking place, shows a distinct ring-like positivity, which became more evident later in development (E15.5) when ABC1-positive cells can be easily assigned to the leptomeningeal sheath (not shown; Halata *et al.*, 1990). By day E13.5, the choroid plexa, now morphologically differentiating, are ABC1-positive and by E15.5 some discrete areas of the ependyma lining the cerebral ventricles also appear strongly ABC1-positive (not shown).

To the second class of signals belong sites which show an intense but transient signal, limited to a tight developmental time window. By day E11.5 the region of the aortic arches appears positive, together with the mesenchyme lining the lung buds and the first bifurcations of the bronchial tree (Figure 1B). Both signals are no longer detectable by E13.5. Again, by E11.5 a longitudinal column of cells in the neural tube (Figure 1B, sagittal section) is detected. These cells are localized in the ventral part of the spinal cord and extend from the ependymal canal into the marginal zone (cross-sections, not shown). This signal is no longer detected by E13.5. Conversely, by day E13, a positive signal appears at the interdigital zone in the hindlimb buds (Figure 1C), most evident in the first interdigital space. Its morphological distribution follows the anatomical development of the digits, being first limited to the distal portion of the interdigital space, and progressing towards the base of the digit by day E13.5/14.5.

ABC1-positive cells in the interdigital zone are macrophages engaged in the engulfment of cell corpses

In order to identify the cells expressing ABC1, an immunohistochemical analysis was focussed on the interdigital zone in the developing hindlimb bud at day E13.5 when the sculpting of the digits due to programmed cell death occurs (Glücksmann, 1951). Two markers were used to detect, in the regressing interdigital space, either the cells undergoing programmed cell death or the cells responsible for their clearance. The precise cytological identification of the latter as macrophages or non-professional phagocytes differentiated locally from fibroblasts is still a matter of discussion (Garcia-Martinez *et al.*, 1993; Hopkinson-Woolley *et al.*, 1994). Since we knew from previous results that ABC1 is expressed by macrophages (Luciani *et al.*, 1994) we tested the reactivity of the interdigital cells with F4/80 antibody, recognizing a membrane determinant of mouse mature macrophages and a potential marker for engulfing cells (Austyn and Gordon, 1981). On the other hand, the distribution of apoptotic cells was

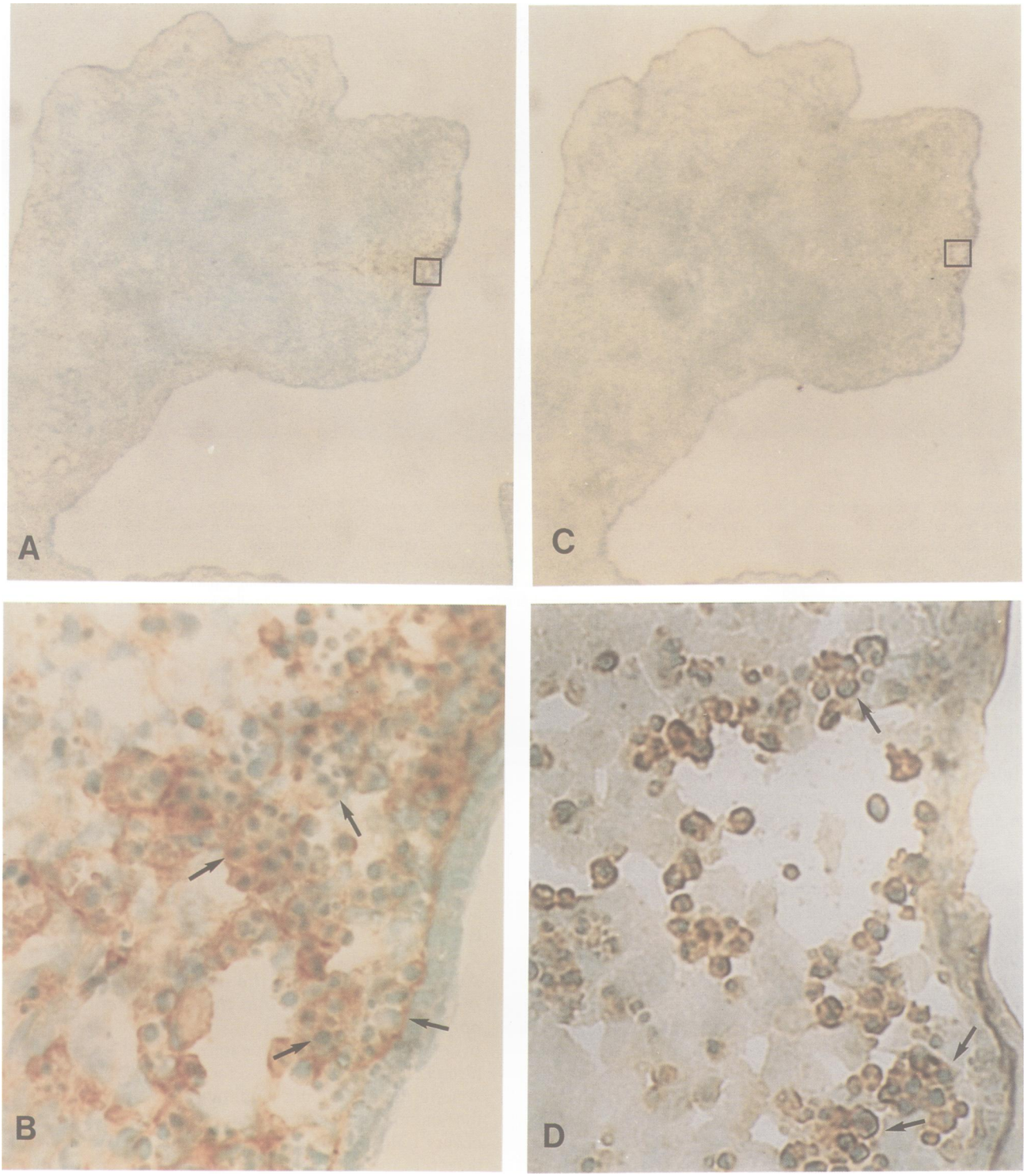

Fig. 2. Immunostaining of sagittal section across the hindlimb bud of E13.5 mouse embryos. F4/80 antigen (**A** and **B**), ABC1 (**C** and **D**) and apoptotic bodies (arrows) show similar patterns of distribution. Both ABC1 and F4/80-positive cells appear to contain several apoptotic bodies. Magnification is ×400 in (B) and (D). The areas identified by the squares in (A) and (C) are enlarged in (B) and (D).

documented *in situ* by digoxigenine–nucleotide tailing of the 3′-OH ends of DNA fragments generated at internucleosomal cleavage sites (TUNEL method, Gavrieli *et al.*, 1992; not shown). Methyl green counterstaining of sections also allowed the detection of apoptotic bodies, which stain hyperchromic with this dye due to the condensation of chromatin (arrowed in Figure 2B and D).

For the detection of ABC1 protein, we used Ab16, a rabbit antiserum directed against the first intracellular ATP binding domain of ABC1, expressed and purified from bacteria as a recombinant protein. This antiserum immunoprecipitated the ABC1 protein, either as an *in vitro* translated product or expressed in *Xenopus* oocytes, and did not cross-react with the 50% identical ABC2 protein (data not shown; Luciani *et al.*, 1994). The specificity of the signal in immunohistochemical analysis was further

confirmed by running parallel assays in the presence of excess recombinant protein; the perfect match between the immunohistochemical and the RNA *in situ* hybridization patterns was taken as an additional confirmation of specificity.

As shown in Figure 2, Ab16, F4/80-stained cells and apoptotic bodies are simultaneously present in the regressing first interdigital space at E13.5 in similar patterns on serial sections across the hindlimb bud. At higher magnification it appears clearly that F4/80-positive cells contain several condensed hyperchromic bodies, as do ABC1-positive cells. The slightly different appearance of the signal is probably due to the different subcellular localization of the determinants detected by the two antibodies. Whereas F4/80 is an extracellular membrane antigen, the epitope recognized by Ab16 on ABC1 protein is intracellular. For comparison, indirect immunofluorescence with Ab16 and F4/80 on thioglycollate-elicited peritoneal macrophages engulfing propidium iodide (PI)-labelled apoptotic thymocytes, is shown in Figure 3. We believe therefore that cells of macrophage origin are responsible for the engulfment of dead cells at the interdigital webs, and that these professional phagocytes express the ABC1 transporter.

As a last point we investigated whether ABC1 expression was detectable in other models of apoptotic cell death such as the massive cell death induced in the thymus by corticosteroid treatment. As recently reported, the vast majority of death in the thymus is detected in the cortical area and most apoptotic bodies are situated within enlarged F4/80-positive macrophages (Surh and Sprent, 1994). It appeared indeed that macrophages engaged in the engulfment of dying thymocytes express both the F4/80 determinant and the ABC transporter ABC1, similarly to the already described situation at the interdigital webs (not shown).

ABC1 is required for engulfment of apoptotic bodies

We then attempted to assess a possible functional requirement for ABC1 during engulfment. To test this, we reconstituted an *in vitro* engulfment assay where thioglycollate-elicited mouse peritoneal macrophages, which express ABC1 (Figure 4A) were challenged with ^{51}Cr-labelled thymocytes induced to apoptosis by sublethal γ irradiation 5–6 h before the assay. This corresponds in fact to 80% viability, assessed by Trypan Blue exclusion and 40% DNA fragmentation, assessed by PI staining, followed by FACS analysis (data not shown; Fadok *et al.*, 1992; Curnow *et al.*, 1994).

To assess the amount of radioactivity specifically due to ingestion of apoptotic thymocytes, the same experiment was carried out at 4°C, when phagocytosis does not take place, or at 37°C with freshly sampled, non-irradiated thymocytes. In both cases macrophage-associated radioactivity never exceeded 35% of the reference engulfment assay (not shown). In a typical experiment macrophages challenged with γ-irradiated thymocytes incorporated 10.3 ± 1.2% at 37°C (average of 12 individual assays), 3.3 ± 1.2% at 4°C (average of eight assays), or 3.5 ± 0.5% in the presence of non-apoptotic thymocytes (average of four assays).

We then reasoned that if ABC1 is indeed required for the ingestion of apoptotic thymocytes, this might be revealed by an antibody-mediated blockade of the ATP binding domain, which is crucial for the function of all ABC transporters. As detailed before, Ab16 is a good candidate as blocking antibody, since it is able to react specifically with the first ATP binding domain of ABC1 in its native conformation. However, since the ATP binding domains are exposed to the cytosol, it was necessary to deliver the antibody intracellularly. We therefore adapted to *ex vivo* macrophages the already described cytosolic loading of macromolecules by osmotic lysis of pinocytic vesicles (Okada and Rechsteiner, 1982). No adverse effect linked to the osmotic shock itself was observed (not shown). In particular, phagocytosis could still be inhibited stereoisomerically by phosphoester derivatives of phosphatidyl-L-serine (Fadok *et al.*, 1992), i.e. pre-incubation with 10^{-3}M phospho-L-serine resulted in an uptake of 40 ± 10% with respect to controls, and with glycerophosphoryl-L-serine of 35 ± 15%, whereas uptake with phospho-D serine was 84 ± 24%. On the other hand, the efficiency of cytosolic loading was documented by the staining of shocked macrophages with a FITC-conjugated secondary antibody (Figure 4B).

Cytosolic loading was then carried out with five different hypertonic mixes, containing medium alone or 10 mg/ml of either affinity-purified Ab16, or Ab526, an antipeptide antiserum recognizing the C-terminal tailpiece of the ABC1 molecule, or Mab 187.1, a mouse monoclonal antibody raised against phosphotyrosines (C.Boyer, unpublished results), or purified rabbit IgG. As summarized in Figure 4C the engulfment ability of apoptotic bodies as measured by monolayer-associated radioactivity can be reduced to 3.7 ± 2%, corresponding to 80.7% inhibition (average percent incorporation of seven individual assays), when the macrophages are preloaded with affinity-purified Ab16 antiserum. Preloading of monolayers with Ab17 antiserum, recognizing the same antigen but raised in a different animal, produced the same results (not shown). Cytoplasmic loading with any of the control immunoglobulins failed to affect the engulfing ability of macrophages, again assessed by the incorporation of radioactivity (Figure 4C). The inhibitory effect driven by Ab16 could, moreover, be titrated (Figure 4D) with half-maximal inhibition at ~3.5 mg/ml. These findings strongly suggest that Ab16 is specifically interfering with phagocytosis in this assay by binding to the functionally crucial ATP binding domain of the ABC1 molecule.

As a last point we explored whether the Ab16-mediated blockade of ABC1 affected phagocytosis in general or was specifically impairing the engulfment of apoptotic cells by testing macrophage ability to ingest labelled yeast cells. After an incubation of 30 min at 37°C macrophage monolayers take up 40 ± 5% (average of four assays) of input radioactivity; this falls to 12.4 ± 3.2% (four assays) when the incubation is carried out at 4°C, but no effect is detected after preloading of macrophages with either Ab16 or RIgG (35 ± 4% and 49 ± 10.8% respectively; four assays; Figure 4D).

ABC1 is highly conserved across evolution

An homology search against the recently reported *C.elegans* database from chromosome III pinpointed the sequence of two computer-predicted ORFs encoding an

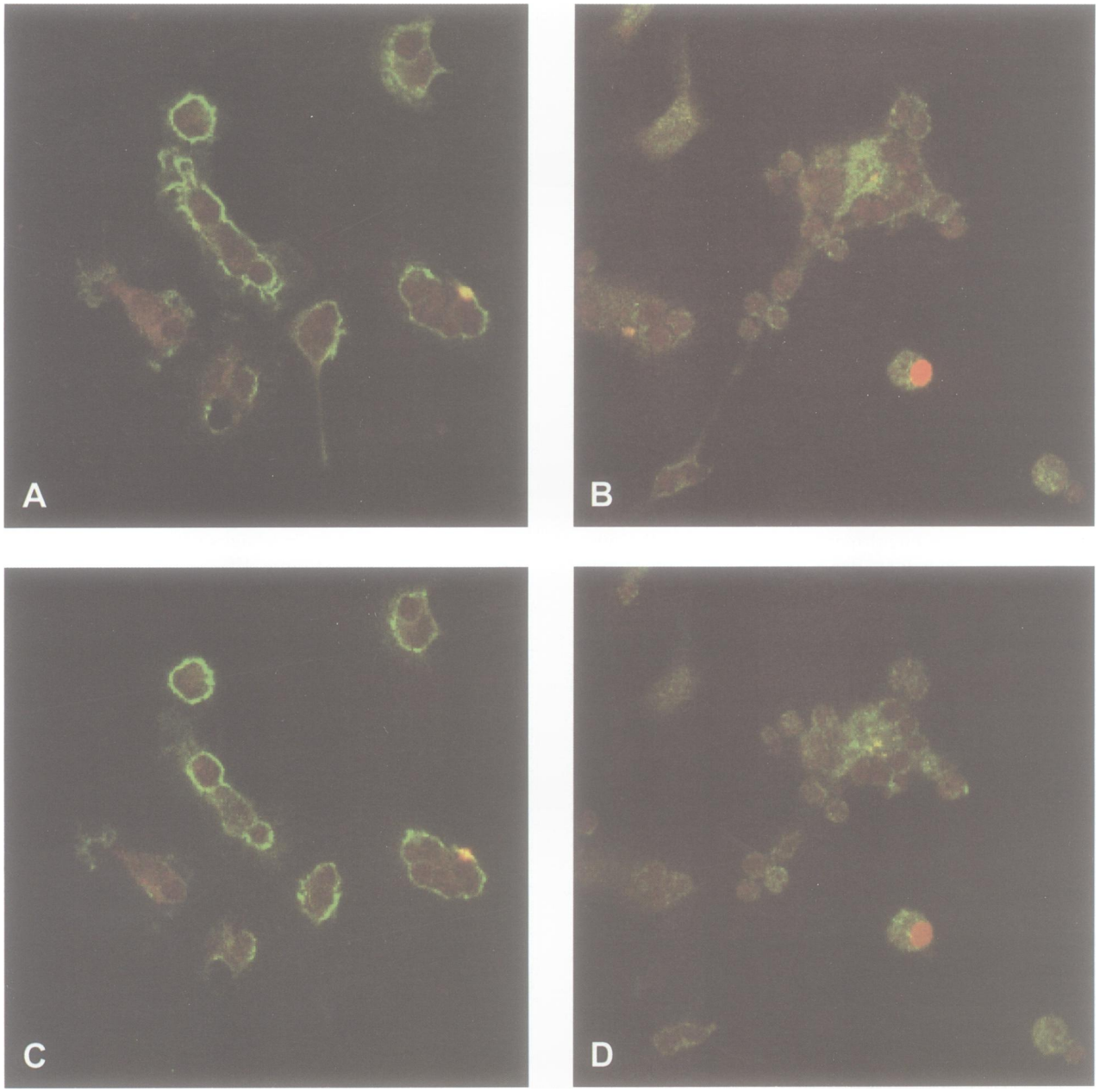

Fig. 3. Confocal immunofluorescence analysis of *in vitro* phagocytosis. Thioglycollate-elicited peritoneal macrophages are allowed to phagocytose PI-stained apoptotic thymocytes for 30 min at 37°C before proceeding to immunodecoration with F4/80 (**A** and **C**), which decorates the external surface of the plasma membrane or Ab16 (**B** and **D**), which stains the cytosolic side of engulfed particles. Two successive confocal sections of ~2.5 μm thickness are shown.

ABC transporter (Wilson *et al.*, 1994). As shown in Figure 5, these putative protein sequences (CEC48B4.PE5 and .PE6) show an overall identity of 30% with the N-terminal and the C-terminal halves of the ABC1 protein sequence. The homology is not evenly distributed along the protein, being highest in the region encompassing the two ATP-binding cassettes, where however it extends clearly beyond the diagnostic motifs shared by all the members of the family. Moreover, the overall homology ranks only slightly lower than that between the mouse and nematode P-glycoproteins (39%). Particularly intriguing, though, is the genomic localization of these ORFs on the 42-kb long cosmid C48B4. Comparative analysis of the physical and genetic maps indeed locates this sequence in close proximity to the *ced-7* locus (Wilson *et al.*, 1994; A.Coulson, Y.Wu and H.R.Horvitz, personal communication). *Ced-7* belongs to the group of genes implicated in the genetic control of programmed cell death in *C.elegans*. It appears to be required—together with at least five other genes—for the engulfment of corpses generated by embryonic cell death (Ellis *et al.*, 1991a,b). *Ced-7* loss of function phenotype results in persistence of corpses, via the functional impairment of a yet-to-be-identified step along the cascade of events required for completion of engulfment.

Discussion

Here, we report on the expression of and functional requirement for the ABC1 transporter in macrophages engaged in

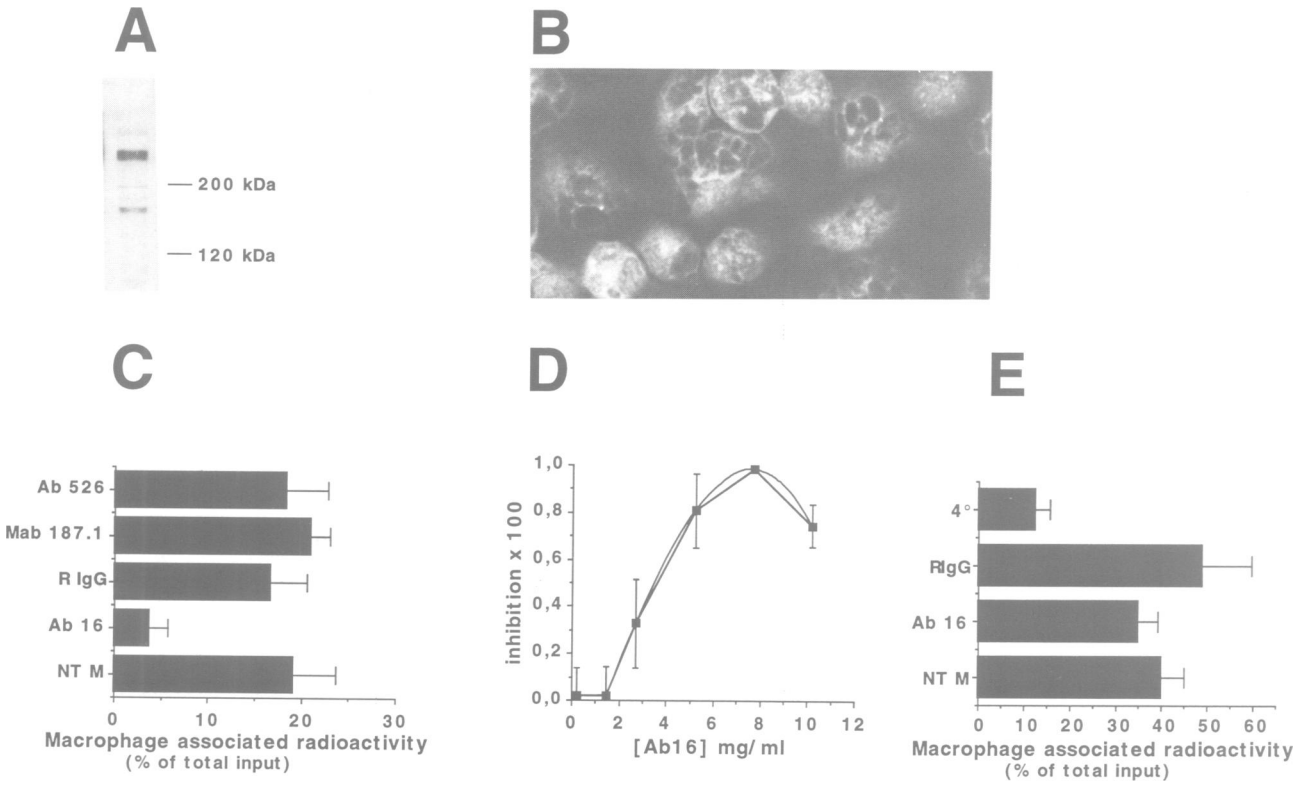

Fig. 4. ABC1 requirement during engulfment of apoptotic thymocytes as assessed by *in vitro* phagocytosis assay. Macrophage-associated radioactivity after incubation with various phagocytic meals at the indicated conditions, is expressed as percent of total input in the phagocytic meal. Percent are the average of multiple experimental points, standard deviation is shown by the thin line. (**A**) Ab16 immunoprecipitation on metabolically labelled thioglycollate-elicited peritoneal macrophages. ABC1 protein product is detected as a band of ~230 kDa. (**B**) Efficacy of cytosolic loading of macromolecules is shown by staining with FITC-secondary antibody on macrophages loaded with RIgG, fixed and permeabilized. (**C**) Inhibition of macrophage ability to engulf apoptotic thymocytes after cytosolic loading with anti-ABC1 antibodies. Bars represent macrophages preloaded with medium alone (NT M), or macrophages preloaded with Ab16, purified rabbit IgG (RIgG), Ab526, or Mab 187.1. Values are: NT M, 19.2 ± 4.4% (12 assays); Ab16, 3.7 ± 2% (seven assays); RIgG, 16.7 ± 3.8% (seven assays); MAb 187.1, 21 ± 2% (four assays); Ab526, 18.4 ± 4.4% (four assays). (**D**) Titration curve of the inhibitory effect of Ab16 preloading on macrophage engulfing ability. Cells were preloaded with increasing concentrations of Ab16 mixed with decreasing concentrations of rabbit immunoglobulins to keep total antibody concentration constant at 10 mg/ml. Results (average of three individual assays) are expressed as percent inhibition with respect to the engulfment ability of macrophages loaded with medium alone. Half-maximal inhibition is obtained at an Ab16 concentration of ~3.5 mg/ml. Values are: Ab16, 0 mg/ml = 13.4 ± 1.6%; 1.25 mg/ml = 13.7 ± 1.7%; 2.5 mg/ml = 9.3 ± 2.6%; 5 mg/ml = 2.9 ± 2%; 7.5 mg/ml = 0.5 ± 0.12%; 10 mg/ml = 3.7 ± 1.2%. (**E**) Phagocytosis of yeast is not inhibited by cytosolic preloading with anti-ABC1 antibody. Bars represent macrophages preloaded with medium alone and incubated with labelled yeast cells for 30 min at 37°C (NT M, 40 ± 5%, four assays) or 4°(4°NT M, 12.4 ± 3.2%, four assays), or macrophages preloaded with Ab16 (35 ± 4%, four assays) or RIgG (49 ± 10.8%, four assays).

the process of engulfment of apoptotic bodies. Analysis of the developmental expression of this transporter by RNA *in situ* hybridization revealed some areas steadily expressing the ABC1 transcript from their initial morphological differentiation and throughout the examined time period. These sites share as a common cytological feature the relative abundance of cells of the monocyte/macrophage lineage (Bleier *et al.*, 1975; Morris *et al.*, 1991), which we know from previous results to express ABC1 (Luciani *et al.*, 1994). Other ABC1-positive sites, however, show a spatial and temporal correlation with the occurrence of developmental cell death. For instance, ABC1 transcript and protein were detected in the hindlimb bud where remodelling of the digits is a well-documented example of developmental death programme. More generally, the whole pattern of transient ABC1 expression is consistent with apoptosis. In fact, by day E11.5 impressive modifications occur in the vascular system leading to the final asymmetry of the aortic arches arterial system. Whereas at earlier stages the six pairs of arches differentiate symmetrically, by E11 to E13 the selective disappearance of the right arches by cell death, followed by the complete removal of the cellular components by phagocytosis, takes place. Cell death is known to occur in close association with branching of the bronchial tree during fetal differentiation of the lungs and, albeit less clearly, the column of ABC1-positive cells in the neural tube might also correlate with death and engulfment processes. In fact in this very region, the occurrence of apoptosis and the active resorption of corpses by invading macrophages has been described in the chick embryo by E4 to E5 (Levi-Montalcini, 1964).

The immunohistochemical analysis of the interdigital zone of the hindlimb bud at E13.5 supports a functional correlation between ABC1 expression and the process of clearance of corpses generated by the death programme, since ABC1-positive cells appear to be phagocytes of macrophage origin engaged in engulfment. A similar ABC1 expression by macrophages in charge of the engulfment and clearance of dead cells was also observed during the intrathymic massive T cell death induced by cytotoxic drugs. The presence of macrophages in areas of cell death, although already reported is still a matter of debate, as

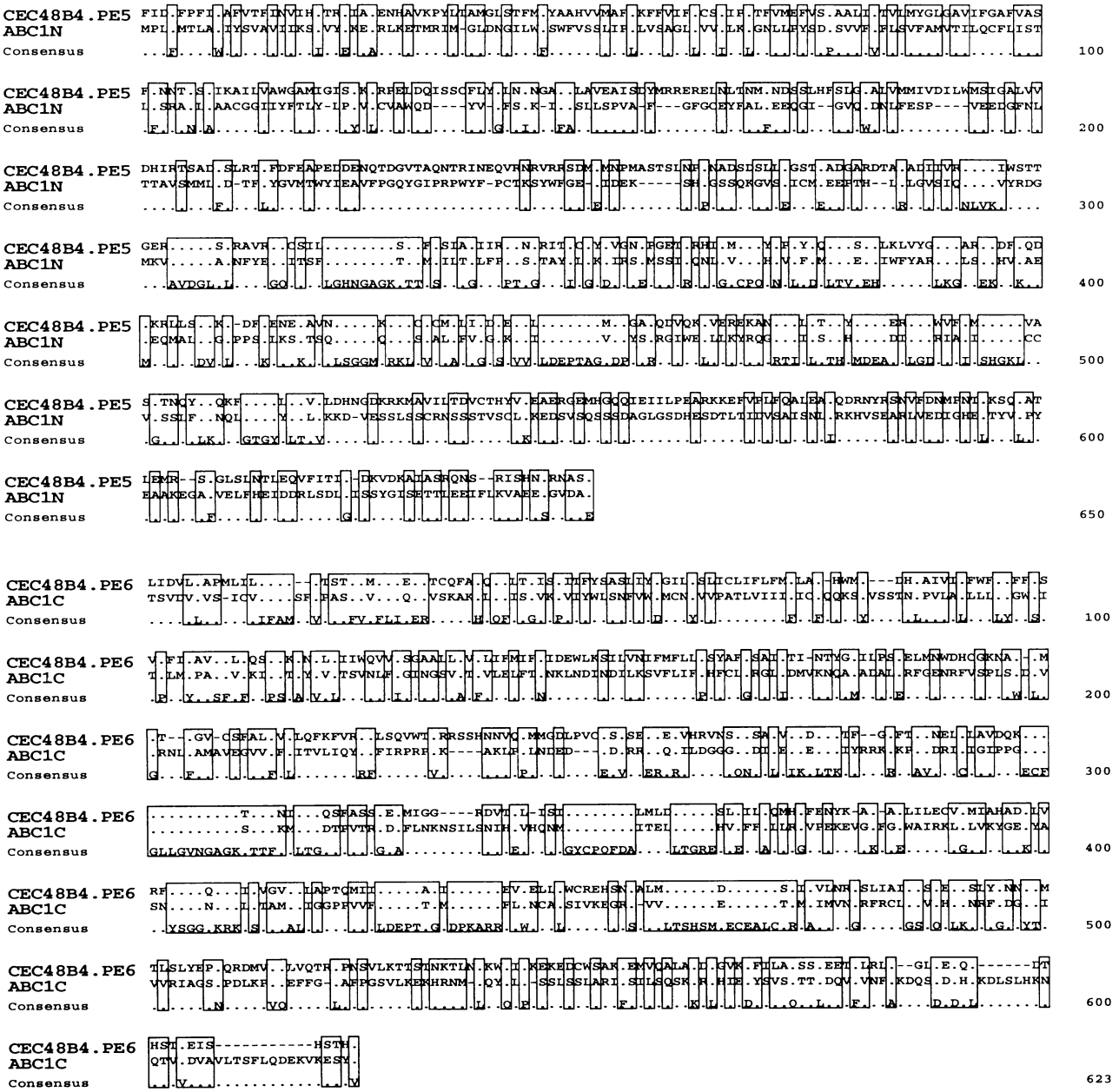

Fig. 5. Sequence alignment according to the Kaneisha algorithm shows 30% amino acid identity between ABC1 and the two *C.elegans* ORFs on cosmid C48B4. Boxed regions are conserved residues.

well as the mechanism of their recruitment. One of the major distinctive features of apoptosis as opposed to necrosis is in fact a complete absence of the inflammatory reaction, usually associated with the massive recruitment of macrophages. For this reason, local differentiation into active phagocytes of non-specialist cells has been frequently evoked as a mechanism at the basis of the rapid disposal of apoptotic corpses. From our data, which are in agreement with previous results (Hopkinson-Woolley *et al.*, 1994; Surh and Sprent, 1994), it appears that professional phagocytes of macrophage origin are present in areas committed to cell death already at or very early after the onset of the death programme. The disposal of corpses is completed quite rapidly as is the clearance of macrophages from the field.

Finally, we could also establish a functional requirement for the ABC1 transporter during the engulfment process, which appears to be specific to the apoptotic nature of the particle to be ingested. The inhibition of apoptotic phagocytosis obtained after cytoplasmic loading with Ab16 is consistent with the functional model for ABC transporters, which predicts that any interference with the ability to bind or hydrolyse ATP would impair the function of the transporter (Hiles *et al.*, 1987; Azzaria *et al.*, 1989; Berkower and Michaelis, 1991; Higgins, 1992). By the same token, the lack of effect after antibody binding to the C-terminal tailpiece provides support to the specificity of the inhibition, while suggesting that this part of the molecule is not essential for function. This is also consistent with the results reported on STE6 transporter, where

engineering of the topologically equivalent region did not alter its function (Berkower and Michaelis, 1991; Kuchler *et al.*, 1993).

Although we could provide evidence for the requirement of an ABC transporter to achieve engulfment, the molecular role of ABC1 is still obscure. Engulfment is a complex and still poorly understood phenomenon (Savill *et al.*, 1993). Its first phase implies the specific recognition of the eliciting particle via the engagement of one or multiple surface receptors and is followed by ingestion *per se* (Berlin and Fera, 1977; Savill *et al.*, 1993). From our results a role of ABC1 in the early recognition or triggering steps elicited by apoptotic cells seems likely, since phagocytosis of yeast is not affected by Ab16 preloading. Most of the data available so far on the genetic control of engulfment derive from the study of the death programme in the nematode *C.elegans*. There, six engulfment genes controlling at least two distinct and parallel processes have been identified. In this context it is highly intriguing to find that the nematode structural homologue of ABC1 transporter lies in close proximity to the *ced-7* genetic locus. *Ced-7* is precisely one of the engulfment genes and its mutation results in persistence of corpses generated by embryonic cell death (Ellis *et al.*, 1991a,b). This similar requirement during engulfment and the coincident genetic localization encourage us to test whether ABC1 and *ced-7* are indeed a pair of structurally and functionally homologous genes. If this turns out to be the case an additional piece of evidence will corroborate the striking evolutionary conservation of genes controlling the death programme (Hengartner and Horvitz, 1994).

Materials and methods

Mice strain and sectioning procedure

Embryos were obtained from timed matings of outbred NMRI mice (CERJ). Embryonic day 0.5 (E0.5) corresponds to the day following the detection of the vaginal plug. At the desired gestational ages, pregnant mice were killed by cervical dislocation and embryos were manually freed from embryonic membranes, fixed in 4% paraformaldehyde in 0.1 M phosphate buffer, pH 7.3, at 4°C overnight, cryoprotected in 15% sucrose, 0.1 M phosphate buffer at 4°C overnight and embedded in Tissue TEK (Miles Laboratories). Cryosections were cut at 8 μm thickness, transferred onto gelatin/chromium(III) potassium sulphate-subbed slides and dried at room temperature. Before *in situ* hybridization or immunohistochemistry slides were post-fixed for 10 min in 4% paraformaldehyde in phosphate buffer at room temperature.

ABC1 probe

The ABC1 probe used for Northern analysis and for *in situ* hybridization was a 1450 bp *PstI–Pst* fragment issued from the central region of ABC1 cDNA (nt 3511–4940 of sequence X75926 deposited in the EMBL database) and subcloned in pBluescript KS (Stratagene, USA).

Northern blot analysis

RNA from whole embryos or cell lines was extracted according to the LiCl–urea method, fractionated on denaturing agarose gels and blotted as already described (Luciani *et al.*, 1994). The gel-purified ABC1-specific probe was labelled to high specific activity by the random priming method; hybridization and washing conditions were as described.

RNA in situ hybridization

ABC1 transcript was detected by the antisense cRNA probe transcribed by T3 RNA polymerase from the above-described DNA template linearized with *Xba*I. A sense cRNA transcribed by T7 RNA polymerase was used as a control for specificity on serial sections. The grain density obtained with the sense probe never exceeded background levels. The probes were labelled by including [^{35}S]UTP in the transcription reaction and hydrolysed to generate 150 bp long fragments. The hybridization procedure was carried out according to Wilkinson and Green (1990). After exposure for 15–20 days slides were developed and counterstained with haematoxylin–eosin, cleared in xylene and mounted in Cytoseal media (Stephens Scientific, Riverdale, NY, USA). Slides were observed through a stereomicroscope (Leica Wild M3Z) equipped with a Volpi darkfield.

Immunohistochemistry

Immunostaining with polyclonal rabbit Ab16 antiserum and the rat mAb reacting with F4/80 antigen (Serotec, UK) (Austyn and Gordon, 1981) was carried out with ABC vectastain kit (Vector Laboratories Inc., USA) according to the manufacturer's instructions. Before immunostaining, the post-fixed slides were treated in 0.3% H_2O_2 in methanol for 30 min to block endogenous peroxidase activity, incubated in 15% normal appropriate serum in PBS for 30 min to block non-specific sites, and briefly trypsinized (0.1% trypsin in PBS) for 30 min at 37°C. After incubations with the primary antibody (anti-ABC1 diluted 1:500 and F4/80 diluted 1:10 in blocking buffer), the assay was carried out following standard protocols, and revealed with DAB peroxidase substrate. The slides were then counterstained with methyl green (0.5% w/v in 0.1 M sodium acetate, pH 4) for 10 min at room temperature, de-stained in butanol and mounted in Cytoseal media (Stephens Scientific). To check for specificity of signal, control slides without primary antibody or in the presence of excess recombinant protein (20 μg/ml) were run in parallel. *In situ* detection of apoptotic bodies was carried out by the Terminal deoxytransferase UTP nucleotide end-labelling method (Apoptag detection kit, Oncor, USA) on post-fixed cryosections, following the manufacturer's instructions.

Production of ABC 1 recombinant protein and antisera Ab16 and Ab526

Since ABC1 protein has a molecular weight >220 kDa and is highly hydrophobic (containing at least 12 transmembrane spanning domains), only a partial construct spanning one of the most hydrophilic regions and corresponding to an intracellular epitope was expressed in bacteria as a recombinant protein. A 1440 bp fragment (nt 2411–3850 of X75926) coding for the whole N-terminal ABC and part of the putative regulatory domain was amplified by the polymerase chain reaction primed with the following oligonucleotides: 5′-GAAGATCTGGAATTCCCAGGCCC-TG-3′ for the forward primer and 5′-AGGAAGCTTTCTTCCA-GGGTGGAGGTC-3′ for the reverse primer. Two nucleotide substitutions were introduced in the reverse primer to generate a *Hin*dIII site. The amplification product was then double-digested with *Bgl*II and *Hin*dIII and cloned in QE9 (Qiagen, USA) vector in frame with a 6× His encoding headpiece and a 3′ stop codon. After checking for the absence of amplification mistakes, competent M15 pRep bacteria were transformed, single colonies expanded and induced with 2 mM IPTG to the expression of the recombinant protein. The presence of the recombinant protein of the expected molecular weight of 45 kDa was checked by Coomassie staining of an analytical SDS–PAGE slab gel of bacterial lysates and the recombinant protein purified by metal affinity chromatography on nickel ions under denaturing conditions (elution by pH gradients in 8 M urea). For immunization purposes, ~100 μg of dialysis renatured protein mixed in equal amounts with complete Freund's adjuvant were injected subcutaneously per animal per boost. Ni-NTA columns loaded with recombinant protein were also used to affinity purify the antiserum following the protocol of Gu *et al.* (1994).

Antiserum Ab526 was generated by immunizing rabbits with a synthetic peptide corresponding to the C-terminal tailpiece of the ABC1 protein sequence (YKNQTVVDVAVLTSFLQDEKVKES). After coupling to BSA according to standard protocols, 100 μg of peptide was used for animal/boost. The antiserum was affinity purified on a small column of peptide following standard protocols. Ab526 is also able to immunoprecipitate *in vitro* translated ABC1 (not shown).

Affinity-purified antibodies were dialysed against water, concentrated by centrifugation on Amicon Centricon 100 filters and lyophilized for subsequent use in cytoplasmic loading.

Preparation of the phagocytic meal and phagocytosis assay

Thioglycollate-elicited peritoneal macrophages (2 ml intraperitoneal injection of thioglycollate medium 4 days previously) were harvested by peritoneal washes from 8–12-week-old B6/CBA mice, extensively washed in complete medium (RPMI 1640 supplemented with 10% FCS) and plated at 2×10^5 cells/well on 96-well microtitre plates. After incubation at 37°C for 2 h, non-adherent cells were eliminated and monolayers incubated overnight at 37°C. Thymocyte suspension was prepared by manual scraping on metallic grids of thymi freshly dissected

from 4-week-old B6/CBA mice, washed in complete medium and labelled with ^{51}Cr (300 μCi/10^8 cells) by incubation for 1 h at 37°C. After additional washes, thymocytes were resuspended at 10^7/ml in complete medium, sublethally γ-irradiated (600 rads) and incubated for 5–6 h at 37°C to allow entrance into apoptosis. One hundred μl aliquots of thymocytes (10^6 cells) were then seeded on macrophages monolayers and incubated at the indicated temperatures for 30 min. To assess background uptake of non-apoptotic thymocytes, macrophages were incubated for 30 min at 37°C with freshly sampled, non-irradiated thymocytes. At the end of the incubation period, non-ingested thymocytes were eliminated by extensive washing in complete medium and macrophage-associated radioactivity counted after lysis of monolayers with 1% SDS.

Phagocytosis of yeast cells

Yeasts (strain US50-18C) were grown to OD_{600} 0.4 by constant agitation in minimal medium at 30°C. Five OD(~3×10^8 cells) were then washed and metabolically labelled for 2 h at 30°C in the presence of 200 μCi of EXPRE^{35}S^{35}S Protein Labelling Mix (NEN-Dupont). After washing in RPMI medium, aliquots of 10^6 cells were seeded on macrophage monolayers and incubated at the indicated temperatures for 30 min. Monolayers associated radioactivity was assessed as described before.

Cytosolic loading of antibodies

Cytosolic loading of antibodies was performed by two successive rounds of osmotic lysis of pinocytic vesicles essentially as described by Okada and Rechsteiner (1982). Briefly, lyophilized affinity-purified antibodies, rabbit-purified IgG, or purified mAb were resuspended at 10 mg/ml in hypertonic medium (RPMI, 0.5 M sucrose, 10% PEG 1000). Aliquots (50 μl) of hypertonic mixes were added to macrophage monolayers for 5 min to allow hypertonic pinocytosis to take place. After a 5 min recovery in complete medium, cells were subjected to hypotonic shock (70% medium, 30% water) for 2 min. A second 5 min recovery was performed before proceeding to the second round of osmotic lysis. Cells were allowed to recover for 30 min at 37°C before the phagocytosis assay. Intra-assay variation was controlled by testing multiple wells per experiment. In the case of Ab16 and rabbit IgG the experiments were repeated twice, for a total of seven individual wells. In order to titrate the inhibitory effect of Ab16, cytosolic loading was performed with hypertonic mixes containing a constant total amount of immunoglobulins (10 mg/ml) obtained by mixing increasing concentrations of Ab16 (0, 1.25, 2.5, 5, 7.5 and 10 mg/ml) with decreasing concentration of purified rabbit IgG. The phagocytosis assay was then performed as before.

Immunofluorescence

Freshly sampled macrophages were plated at 4×10^5 on glass coverslips and incubated overnight at 37°C. Indirect immunofluorescence was performed according to standard protocols for surface antigens (F4/80) or intracellular antigens (Ab16) (Celis, 1994). To assess cytosolic loading of the antibody, cells were fixed, permeabilized and then stained with the secondary FITC-conjugated anti-rabbit antibody (Immunotech, France). Images were analysed on a Leica confocal microscope (model TCS 4D). For the morphological analysis of *in vitro* phagocytosis, the assay was carried out as described before except that the thymocytes were unlabelled and stained with PI (0.5 μg/ml in complete medium for 10 min) just before the assay.

Immunoprecipitation

Freshly sampled macrophage monolayers were metabolically labelled overnight at 37°C in the presence of 400 μCi of EXPRE^{35}S^{35}S Protein Labelling Mix (NEN-Dupont) lysed in 1% Triton X-100, 100 mM Tris–HCl (pH 8), 100 mM NaCl, 10 mM EDTA at 4°C and immunoprecipitated with Ab16 following standard protocols (Celis, 1994).

Sequence comparison

Sequence analysis was performed by the Bysance system of programs and databases implemented on a VAX 8530 of the Centre Interuniversitaire de Traitment de l'Information, Paris France. The Kaneisha algorithm was used for pair-wise alignment.

Acknowledgements

The authors wish to thank H.R.Horvitz, A.Coulson and Y.Wu for having provided useful information on the *C.elegans* genetic map, J.F.Brunet and P.Golstein for helpful discussion, C.Goridis, L.Leserman, B.Malissen and A.M.Schmitt-Verhulst for critically reading the manuscript. Special thanks are given to C.Boyer, who provided the 187.1 antibody, to A.K.Simon for help with FACS analysis, and to M.Fathallah for his help with confocal imaging. This work has been supported by institutional grants from INSERM and CNRS and by specific grants from ARC and LNLC.

References

Austyn,J.M. and Gordon,S. (1981) F4/80, a monoclonal antibody directed specifically against the mouse macrophage. *Eur. J. Immunol.*, **11**, 805–815.

Azzaria,M., Schurr,E. and Gros,P. (1989) Discrete mutations in the predicted nucleotide binding sites of the *mdr-1* gene abolish its ability to confer multidrug resistance. *Mol. Cell. Biol.*, **9**, 5289–5297.

Berkower,C. and Michaelis,S. (1991) Mutational analysis of the yeast a-factor transporter STE6, a member of the ATP binding cassette (ABC) protein superfamily. *EMBO J.*, **10**, 3777–3785.

Berlin,R.D. and Fera,J.P. (1977) Changes in membrane microviscosity associated with phagocytosis: effects of colchicine. *Proc. Natl Acad. Sci. USA*, **74**, 1072–1076.

Bleier,R., Albrecht,R. and Cruce,J.A.F. (1975) Supraependymal cells of hypothalamic third ventricle: identification as resident phagocytes of the brain. *Science*, **189**, 299–301.

Celis,J.E. (1994) *Cell Biology. A Laboratory Handbook*. Academic Press, San Diego.

Curnow,S.J., Barad,M., Brun-Roubereau,N. and Schmitt-Verhulst,A.M. (1994) Flow cytometric analysis of apoptotic and non apoptotic T-cell receptor-transgenic thymocytes following *in vitro* presentation of antigen. *Cytometry*, **16**, 41–48.

De la Salle,H. *et al.* (1994) Homozygous human TAP peptide transporter mutation in HLA class I deficiency. *Science*, **265**, 237–241.

Doige,C.A. and Ames,G.F.-L. (1993) ATP-dependent transport systems in bacteria and humans: relevance to cystic fibrosis and multidrug resistance. *Annu. Rev. Microbiol.*, **47**, 291–319.

Ellis,R.E., Jacobson,D.M. and Horvitz,H.R. (1991a) Genes required for the engulfment of cell corpses during programmed cell death in *Caenorhabditis elegans*. *Genetics*, **129**, 79–94.

Ellis,R.E., Yuan,J. and Horvitz,H.R. (1991b) Mechanisms and functions of cell death. *Annu. Rev. Cell Biol.*, **7**, 663–698.

Fadok,V., Voelker,D.R., Campbell,P.A., Cohen,J.J., Bratton,D.L. and Henson,P.M. (1992) Exposure of phosphatidylserine on the surface of apoptotic lymphocytes triggers specific recognition and removal by macrophages. *J. Immunol.*, **148**, 2207–2216.

Garcia-Martinez,V., Macias,D., Ganan,Y., Garcia-Lobo,J.M., Francia, M.V., Fernandez-Teran,M.A. and Hurle,J.M. (1993) Internucleosomal DNA fragmentation and programmed cell death (apoptosis) in the interdigital tissue of the embryonic chick leg bud. *J. Cell Sci.*, **106**, 201–208.

Gartner,J., Moser,H. and Valle,D. (1992) Mutations in the 70K peroxisomal membrane protein gene in Zellweger syndrome. *Nature Genet.*, **1**, 16–22.

Gavrieli,Y., Sherman,Y. and Ben-Sasson,S.A. (1992) Identification of programmed cell death *in situ* via specific labeling of nuclear DNA fragmentation. *J. Cell Biol.*, **119**, 493–501.

Glücksmann,A. (1951) Cell deaths in normal vertebrate ontogeny. *Biol. Rev.*, **26**, 59–86.

Gottesman,M.M. and Pastan,I. (1992) Biochemistry of multidrug resistance mediated by the multidrug transporter. *Annu. Rev. Biochem.*, **62**, 385–428.

Gu,J., Stephenson,C.G. and Iadarola,M.J. (1994) Recombinant proteins attached to a nickel-NTA column: use in affinity purification of antibodies. *Biotechniques*, **17**, 257–262.

Halata,Z., Grim,M. and Christ,B. (1990) Origin of spinal cord meninges, sheaths of peripheral nerves, and cutaneous receptors including Merkel cells. *Anat. Embryol.*, **182**, 529–537.

Hengartner,M.O. and Horvitz,H.R. (1994) Programmed cell death in *Caenorhabditis elegans*. *Curr. Opin. Genet. Dev.*, **4**, 581–586.

Higgins,C.F. (1992) ABC transporters: from microorganisms to man. *Annu. Rev. Cell Biol.*, **8**, 67–113.

Hiles,I.D., Gallagher,M.P., Jamieson,D.J. and Higgins,C.F. (1987) Molecular characterization of the oligopeptide permease of *S. typhimurium*. *J. Mol. Biol.*, **195**, 125–142.

Hopkinson-Woolley,J., Hugues,D., Gordon,S. and Martin,P. (1994) Macrophage recruitment during limb development and wound healing in the embryonic and fetal mouse. *J. Cell Sci.*, **107**, 1159–1167.

Kaufman,M.H. (1992) *The Atlas of Mouse Development*. Academic Press, San Diego, CA.

Kuchler,K., Dohlman,H.G. and Thorner,J. (1993) The a-factor transporter (*STE6* gene product) and cell polarity in the yeast *Saccharomyces cerevisiae*. *J. Cell Biol.*, **120**, 1203–1215.

Levi-Montalcini,R. (1964) Events in the developing nervous system. *Prog. Brain Res.*, **4**, 1–29.

Luciani,M.F., Denizot,F., Savary,S., Mattei,M.G. and Chimini,G. (1994) Cloning of two novel ABC transporters mapping on human chromosome 9. *Genomics*, **21**, 150–159.

McGrath,J.P. and Varshavsky,A. (1989) The yeast STE6 encodes a homologue of the mammalian multidrug resistance P-glycoprotein. *Nature*, **340**, 400–404.

Morris,L., Graham,C.F. and Gordon,S. (1991) Macrophages in haemopoietic and other tissues of the developing mouse detected by the monoclonal antibody F4/80. *Development*, **112**, 517–526.

Mosser,J., Douar,A.-M., Sarde,C.O., Kioschis,P., Feil,R., Moser,H., Poustka,A.-M., Mandel,J.L. and Aubourg,P. (1993) Putative X-linked adrenoleucodystrophy gene shares unexpected homology with ABC transporters. *Nature*, **361**, 726–730.

Okada,C.Y. and Rechsteiner,M. (1982) Introduction of macromolecules into cultured mammalian cells by osmotic lysis of pinocytic vesicles. *Cell*, **29**, 33–41.

Riordan,J.R. *et al.* (1989) Identification of the cystic fibrosis gene: cloning and characterization of complementary DNA. *Science*, **245**, 1066–1073.

Ruetz,S. and Gros,P. (1994) Phosphatidylcholine translocase: a physiological role for the *mdr2* gene. *Cell*, **77**, 1071–1081.

Savill,J., Fadok,V., Henson,P. and Haslett,C. (1993) Phagocyte recognition of cells undergoing apoptosis. *Immunology Today*, **14**, 131–135.

Smit,J.J.M. *et al.* (1993) Homozygous disruption of the murine *mdr2* P-glycoprotein gene leads to a complete absence of phospholipid from bile and to liver disease. *Cell*, **75**, 451–462.

Surh,C.D. and Sprent,J. (1994) T-cell apoptosis detected *in situ* during positive and negative selection in the thymus. *Nature*, **372**, 100–103.

Valle,D. and Gartner,J. (1993) Penetrating the peroxisome. *Nature*, **361**, 682–683.

Wilkinson,D.G. and Green,J. (1990) *In situ* hybridization and three-dimensional reconstruction of serial sections. In Copp,A.J. and Cockroft,D.L. (eds), *Postimplantation Mammalian Embryos: A Practical Approach*. IRL Press, Oxford, pp. 155–171.

Wilson,R. *et al.* (1994) 2.2 Mb of contiguous nucleotide sequence from chromosome III of *C. elegans*. *Nature*, **368**, 32–38.

Received on May 11, 1995; revised on October 4, 1995